The American Journal of Pathology, Vol. 174, No. 3, March 2009

DOI: 10.2353/ajpath.2009.080501

Tumorigenesis and Neoplastic Progression

Spontaneous Metastasis of Prostate Cancer Is Promoted by Excess Hyaluronan Synthesis and Processing

Alamelu G. Bharadwaj,* Joy L. Kovar,† Eileen Loughman,* Christian Elowsky,* Gregory G. Oakley,‡ and Melanie A. Simpson*

From the Department of Biochemistry, University of Nebraska, LI-COR Biosciences,† the Department of Oral Biology,‡ University of Nebraska Medical Center College of Dentistry, Lincoln, Nebraska*

Accumulation of extracellular hyaluronan (HA) and its processing enzyme, the hyaluronidase Hyal1, predicts invasive, metastatic progression of human prostate cancer. To dissect the roles of hyaluronan synthases (HAS) and Hyal1 in tumorigenesis and metastasis, we selected nonmetastatic 22Rv1 prostate tumor cells that overexpress HAS2, HAS3, or Hyal1 individually, and compared these cells with co-transfectants expressing Hyal1 + HAS2 or Hyal1 + HAS3. Cells expressing only HAS were less tumorigenic than vector control transfectants on orthotopic injection into mice. In contrast, cells co-expressing Hyal1 + HAS2 or Hyal1 + HAS3 showed greater than sixfold and twofold increases in tumorigenesis, respectively. Fluorescence and histological quantification revealed spontaneous lymph node metastasis in all Hyal1 transfectant-implanted mice, and node burden increased an additional twofold when Hyal1 and HAS were co-expressed. Cells only expressing HAS were not metastatic. Thus, excess HA synthesis and processing in concert accelerate the acquisition of a metastatic phenotype by prostate tumor cells. Intratumoral vascularity did not correlate with either tumor size or metastatic potential. Analysis of cell cycle progression revealed shortened doubling times of Hyal1-expressing cells. Both adhesion and motility on extracellular matrix were diminished in HA-overproducing cells; however, motility was increased twofold by Hyal1 expression and fourfold to sixfold by Hyal1/HAS co-expression, in close agreement with observed metastatic potential. This is the first comprehensive examination of these enzymes in a relevant prostate cancer microenvironment. ***(Am J Pathol 2009, 174:1027–1036; DOI: 10.2353/ajpath.2009.080501)***

Prostate tumors detected early are often managed effectively by surgical resection and/or hormone ablation therapy. However, a significant percentage of tumors resume growth in the absence of androgens.[1] The transformation from androgen- dependent to androgen-independent prostate cancer is incompletely understood, and such tumors are typically highly aggressive. Progression of human prostate cancer to invasive and/or metastatic growth is accompanied by significant deposition and accumulation of hyaluronan (HA) within the tumors. HA is a large secreted glycosaminoglycan polymer that normally functions in motility and cell transformation during development and wound healing.[2–5] Matrices rich in HA tend to be comparatively deficient in covalently cross-linked fibrous protein networks,[6] more gel-like and less organized, thus altering the normal architecture of the tissue matrix by increasing its permeability. This undermining of tissue structural integrity may be permissive to pathological cell proliferation and movement, particularly in cancer.[4] Furthermore, its role as an adhesion and migration substrate for cells in development may translate to enhanced metastatic potential of cells bearing surface-associated HA.

Many previous reports have documented the involvement of HA and its receptors in prostate cancer progression.[7–13] In human prostate cancer patients, high levels of HA correlated with locally invasive tumor growth and prostate-specific antigen recurrence, both independent indicators of negative prognosis.[7] Quantification of the HA processing hyaluronidase, Hyal1, was demonstrated to be predictive of continued disease progression after

Supported by the US Army (Prostate Cancer Research Grant DAMD 04-1-0041 to M.A.S.) and the National Institutes of Health (grants R01 CA106584 and NCRR P20 RR018759 to M.A.S.).

Accepted for publication November 24, 2008.

Address reprint requests to Dr. Melanie A. Simpson, Associate Professor, Department of Biochemistry, University of Nebraska–Lincoln, N246 Beadle Center, Lincoln, NE 68588-0664. E-mail: msimpson2@unl.edu.

hormone ablation therapy,[11] which is normally effective in early-stage prostate cancers.

Our previous research has differentially implicated HA synthase (HAS) isozymes HAS2 and HAS3, both of which produce HA polymers, in conjunction with Hyal1, which processes HA polymers to oligomers, in aspects of aggressive tumor progression.[14–19] In particular, excessive cellular HA retention and autocrine processing was predicted to promote metastasis. Among cultured human prostate tumor cell lines, elevated HA production was found specifically in aggressive, metastatic cells, in which HAS2 and HAS3 isozymes were up-regulated ≈3-fold and ≈30-fold, respectively.[17] Suppression of HAS2 and/or HAS3 expression by stable antisense RNA reduced the synthesis and cell surface retention of HA,[18] and inhibited primary subcutaneous or intraprostatic growth.[19] Reduced primary tumor growth was associated with comparable apoptotic and proliferative fractions in culture and in tumors, but virtually no vascularization of tumors. These results implicate HA, and specifically HAS2 and HAS3, in tumor angiogenesis, as well as intrinsic growth rate modulation. Interestingly, exogenous HA addition to knock-down cells on injection restored subcutaneous tumor growth and angiogenesis, implying the existence of a tumor or stromal factor (ie, a hyaluronidase) that could modulate effects of HA in trans, with the same malignant outcome. We hypothesized that concerted action of these enzymes at elevated levels in prostate tumors would facilitate aggressive primary tumor growth by potentiating tumor cell proliferation and vascularization of tumors.

To segregate the effects of HA synthesis by the HAS enzymes from HA turnover by Hyal1, we previously selected 22Rv1 prostate adenocarcinoma cells to stably overexpress Hyal1, HAS2, or HAS3, and to co-express Hyal1 + HAS2 or Hyal1 + HAS3. Growth kinetics in culture and in subcutaneous murine tumors were compared.[14–16] HAS2 expressed alone or co-expressed with Hyal1 in 22Rv1 tumor cells increased subcutaneous growth and vascularization of tumors. In contrast, overexpression of HAS3, which conferred 20-fold higher HA production than GFP controls and fivefold more than HAS2 transfection, diminished subcutaneous tumor growth and vascularization. Because the subcutaneous microenvironment is already a site of abundant HA turnover, we reasoned that the physiologically relevant microenvironment of the prostate, normally a site of low HA production and turnover, might be impacted differently by tumor cells with these properties, in a manner more representative of the human disease. Therefore, the goal of this study was to define the respective roles of HA synthases and hyaluronidases for the first time in orthotopic growth and metastasis of prostate tumor cells, and identify the underlying cellular processes affected.

Materials and Methods

Cell Culture and Reagents

22Rv1 human prostate adenocarcinoma cells from American Type Culture Collection (Rockville, MD) were cultured in RPMI 1640/10% fetal bovine serum as recommended. Stable transfectants were maintained in standard media supplemented with 1.5 mg/ml of G418. Biotinylated HA binding protein was from Seikagaku (Tokyo, Japan). Anti-mouse CD31-phycoerythrin conjugate was from BD Biosciences Pharmingen (Franklin Lakes, NJ). Collagen type IV was from Fisher Biosciences (Pittsburgh, PA). Standard mouse chow and purified maintenance diet (AIN-93M) were obtained from Harlan Teklad (Madison, WI). IRDye 800CW EGF was supplied by LI-COR Biosciences (Lincoln, NE). The Odyssey infrared imaging system was also provided by LI-COR Biosciences.

Orthotopic Injection

Male NOD/SCID mice (The Jackson Laboratory, Bar Harbor, ME) were cared for and maintained under the supervision and guidelines of the University of Nebraska–Lincoln Institutional Animal Care and Use Committee. Six-week-old mice were anesthetized with 2% isoflurane and injected in the left lobe of the dorsal prostate with 1×10^5 22Rv1 transfectant cells (seven mice per group) suspended in serum-free medium. Tumor growth was tracked by optical imaging at 2, 4, and 6 weeks, each time 3 days after intravenous injection of 1 nmol IRDye 800CW EGF targeting agent. Control animals injected only once at the endpoint confirmed that no differences in tumor size occurred within animal groups as a result of longitudinal exposure to the agent. In addition, tumor weights and lymph node hematoxylin and eosin (H&E) staining were repeated with identical results in a second experiment using eight animals per group, in which imaging was not used.

Near Infrared Imaging of Tumors and Lymph Nodes

Near infrared fluorescence imaging in live animals was performed with a prototype small animal imager as previously described.[15] Images were acquired and analyzed with Wasabi software from Hamamatsu Photonics (Hamamatsu City, Japan) or Adobe Photoshop (Adobe Systems Inc., San Jose, CA). For longitudinal tracking, shaved anesthetized mice were imaged in a sealed, sterilized portable compartment, circulated with HEPA-filtered air.

Statistical Analysis of Animal Fluorescence Data

Images analyzed in a longitudinal series for each mouse were normalized using the same look-up table with a common minimum and maximum value. Signal-to-noise ratio was calculated using the following formula:

$$\mathrm{SNR} = \frac{((\text{Maximum tumor intensity}) - (\text{Mean background intensity}))}{\text{Standard deviation of mean background}}$$

Regions of interest with identical areas were quantified for total pixel and mean pixel values. The SD of mean backgrounds was calculated using three to five regions

of interest. Statistical variance among tumor wet weights and lymph node metastatic burden was calculated by one-way analysis of variance comparing each group mean to the GFP control group. Group means were evaluated for significance at probability values of 0.05 and 0.01.

Immunohistochemistry and Immunofluorescence

HA content and vascularization of tumors were detected as described previously.[16,19] Briefly, tumors were divided in halves. One half was formalin-fixed and embedded in paraffin. The other half was snap-frozen in OCT compound. For HA detection, paraffin-embedded tumors were sectioned, dewaxed, incubated with 3 μg/ml of biotinylated HA binding protein in phosphate-buffered saline/1% bovine serum albumin overnight at 4°C, and developed using the Vectastain ABC kit (Vector Laboratories, Irvine, CA). Sections were counterstained with Meyer's hematoxylin. White light images were collected at ×200 magnification. Vascularization of the tumors was assessed in acetone-fixed frozen sections (8 μm thickness) by antibody staining for CD31 as described previously.[14,16,19,21]

Angiogenesis Quantification

CD31-phycoerythrin-conjugated antibody staining of frozen sections was visualized by fluorescence microscopy. Ten random sections from each of three tumors per cell line were digitally photographed with 5 seconds of exposure time, saved as TIF files, and processed. Average pixel density for each transfectant tumor section was normalized to the average pixel density for untransfected tumor sections. One-way analysis of variance was used to determine whether variance in total vascular pixel density among the 30 images for each transfectant tumor group was significantly different from 30 images of the GFP control transfectant tumors. Significance was evaluated at probabilities of 0.05 and 0.01.

Cell Cycle Analysis

Transfectant tumor cells cultured in standard medium were trypsinized, washed, fixed overnight at −20°C, and stained overnight at 4°C with propidium iodide containing RNase. Cells were analyzed by flow cytometry using a FACSArray Bioanalyzer (BD Biosciences) with ModFit software. Percentages of each transfectant cell type in respective phases of the cycle were plotted (asynchronous). To synchronize cells, which were not susceptible to serum synchronization, we treated for 24 hours with 0.2 μmol/L nocodazole, a mitotic inhibitor. Treated cells were segregated into two pools, one of which was continually exposed to nocodazole (arrested) and one from which nocodazole was removed for 24 hours before assay (arrested and released). Cells were analyzed similarly to the asynchronous population. Statistical significance at each time point was assessed by one-way analysis of variance relative to GFP control values.

Extracellular Matrix Adhesion

Microplates were precoated with type IV collagen in serially diluted doses for 1 hour at 25°C and blocked with 3% bovine serum albumin. Subconfluent cells were released with 1 mmol/L ethylenediaminetetraacetic acid, washed, resuspended in adhesion medium (serum-free RPMI 1640 containing 20 mmol/L HEPES, pH 7.2, and 1% bovine serum albumin), and labeled with calcein-AM (25 μg/10^6 cells, 20 minutes at 37°C). Labeled cells (10^4 cells/well) were incubated in quadruplicate wells of the precoated plates for 2 hours at 37°C. Nonadherent cells were removed with three gentle washes in adhesion medium. Remaining adherent cells were lysed, fluorescence was quantified, and the percentage of adherent cells relative to the input number was calculated from a standard curve of each labeled cell culture. Significance was determined by one-way analysis of variance.

Motility

Motility of the transfectants was assayed using a 48-well modified Boyden chamber (Neuroprobe, Inc., Gaithersburg, MD). Briefly, single cell suspensions (20,000 cells/well) in serum-free RPMI were placed in quadruplicate into the upper wells of the chamber with type IV collagen (25 μmol/L) in the lower well. Membranes used to separate the wells were 8 μm pore size. After 20 hours of incubation at 37°C in a humidified chamber, membranes were fixed and stained with Diff-Quik (Fisher Biosciences), and placed with migrated side down on a glass microscope slide. Nonmigrated cells were wiped away with a cotton swab. Remaining migrated cells were counted at ×150 magnification in five random fields per well and plotted as mean ± SEM of average migrated cells per well. Significance was determined by one-way analysis of variance.

Results

To examine the role of HA metabolic enzymes in prostate tumorigenesis and metastasis, we performed orthotopic injections in male NOD/SCID mice. From the orthotopic site, we previously determined that 22Rv1 cells were nonmetastatic but could be induced to metastasize to the para-aortic lymph nodes within a 6-week time course on overexpression of Hyal1.[15] Growth of tumors was monitored for 6 weeks by near infrared optical imaging using fluorescent dye conjugated to EGF. At 2-week intervals, images were collected and analyzed for total lower abdominal fluorescence at signal to noise ratios of >3 standard deviations above background (Figure 1A). Differential growth rates among the tumors were evident by week 2, with several consistent trends emerging by week 4. At 6 weeks, prostates were harvested and weighed (Figure 1B). As we observed previously, Hyal1 overexpression

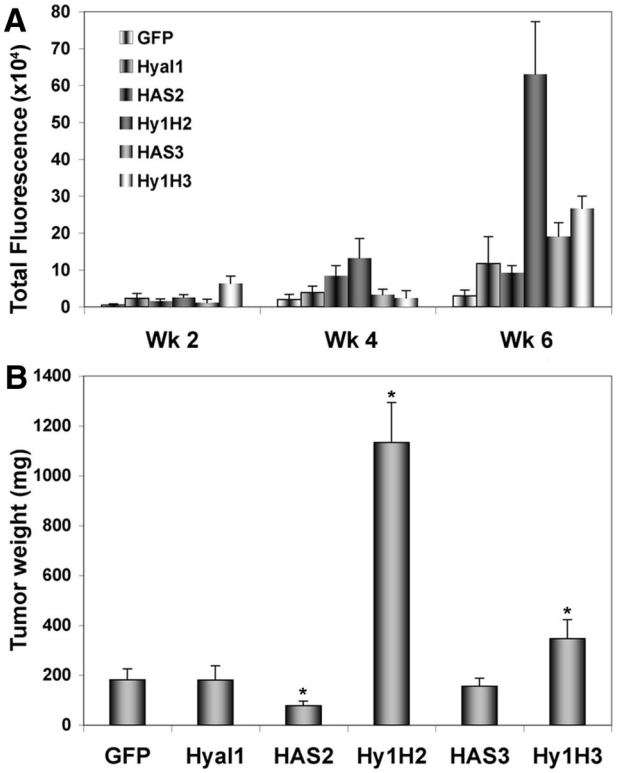

Figure 1. Orthotopic prostate tumorigenesis is enhanced by co-expression of HA-synthesizing and HA-turnover enzymes. Single cell suspensions of transfected cell lines as indicated were injected in 10 μl of serum-free RPMI to the dorsal prostate of male NOD/SCID mice (seven per group, repeated in triplicate). **A:** Tumor growth was monitored longitudinally at 2-week intervals by near infrared optical imaging. Mice were imaged 72 hours after an intravenous injection of IRDye 800CW EGF (1 nmol). Images were analyzed for total tumor fluorescence detected at signal to noise ratios of >5 SDs above background. **B:** At 6 weeks after surgery, after the final image capture, animals were sacrificed and tumors were harvested and weighed. Plotted is the mean tumor wet weight ± SEM for all mice; $^*P < 0.01$.

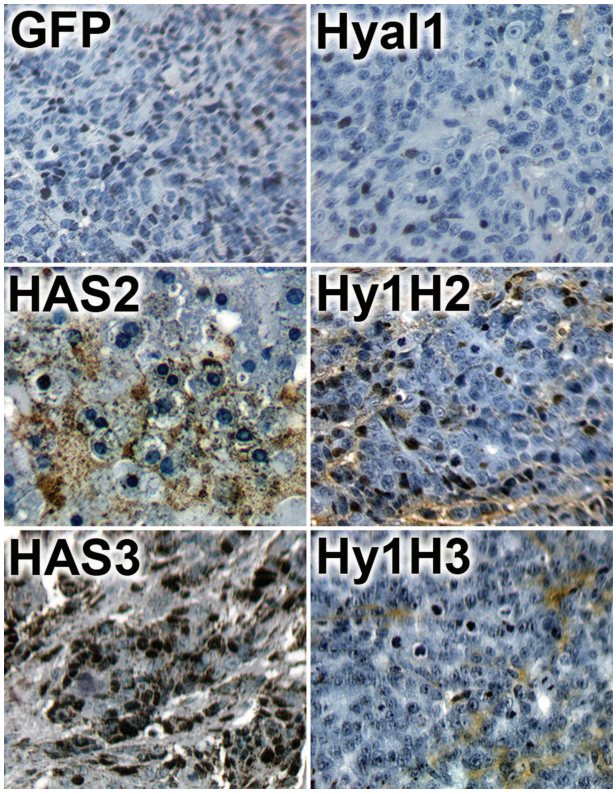

Figure 2. HA content of orthotopic tumor sections. Formalin-fixed, paraffin-embedded tumors were sectioned and stained with biotinylated HA binding protein, followed by detection with streptavidin-conjugated HRP and diaminobenzidine precipitation to visualize HA content. Sections were counterstained with hematoxylin and representative fields were digitally photographed at ×200 magnification.

alone did not alter endpoint tumor size. Either HAS2 or HAS3 expression suppressed intraprostatic 22Rv1 growth, with only ≈25% (HAS2) and ≈58% (HAS3) of injected animals bearing tumors. Of the resulting tumors, the overexpression of either HAS2 or HAS3 also reduced tumor size, although statistical significance for HAS3 was not established ($P = 0.06$). In contrast, concurrent expression of HAS2 and Hyal1 or HAS3 and Hyal1 increased tumorigenesis approximately sixfold and twofold, respectively. Suppressed growth of HAS-overexpressing cells is consistent with previously characterized intrinsic growth rates of the respective cell lines in culture.[14,16] However, the increased tumorigenic potential of Hyal1 + HAS co-expressing cells in the otherwise HA-deficient prostatic environment exceeds the growth potential predicted by the intrinsic kinetics in culture, suggesting additional parameters are important for prostate colonization of the transfectants.

HA content of prostate tumors was evaluated by probing paraffin-embedded sections with a specific HA binding protein (Figure 2). As expected, neither control GFP nor Hyal1 tumor sections stained appreciably for HA. However, the HAS2 and HAS3 tumors exhibited abundant HA accumulation at the cell surface and pooled within regions of the tumor matrix. Importantly, co-expression of either HAS isozyme with Hyal1 markedly reduced HA accumulation within the tumors. These observations are consistent with growth suppression by HA in high concentrations produced by HAS, and with relief from growth suppression on Hyal1-mediated HA turnover.

One potential explanation for increased tumor growth could be that Hyal1-catalyzed degradation of HA may occur in the extracellular space,[22] giving rise to low molecular weight HA oligosaccharides with angiogenic potential,[23] and thereby promoting vascularization of the tumors. Therefore, we quantified the vascular density of the tumor sections by probing with anti-CD31 (Figure 3, graph). In contrast to what we expected, vascularization of prostate tumors arising from each of the cell lines was modestly increased by HAS-mediated HA production but was unaltered by concurrent HA processing. Interestingly, scrutiny of the raw images for each tumor analyzed (Figure 3, top) revealed a notable difference in the morphology of the intratumoral vessels. Tumors arising from HAS-overexpressing cells contained vasculature of more robust appearance as judged by the intensity of fluorescence staining. They were also more sparsely distributed within the tumor. Vessels occurring within GFP control tumors and all Hyal1-expressing transfectant lines (Figure 3, right column) were significantly finer in appearance

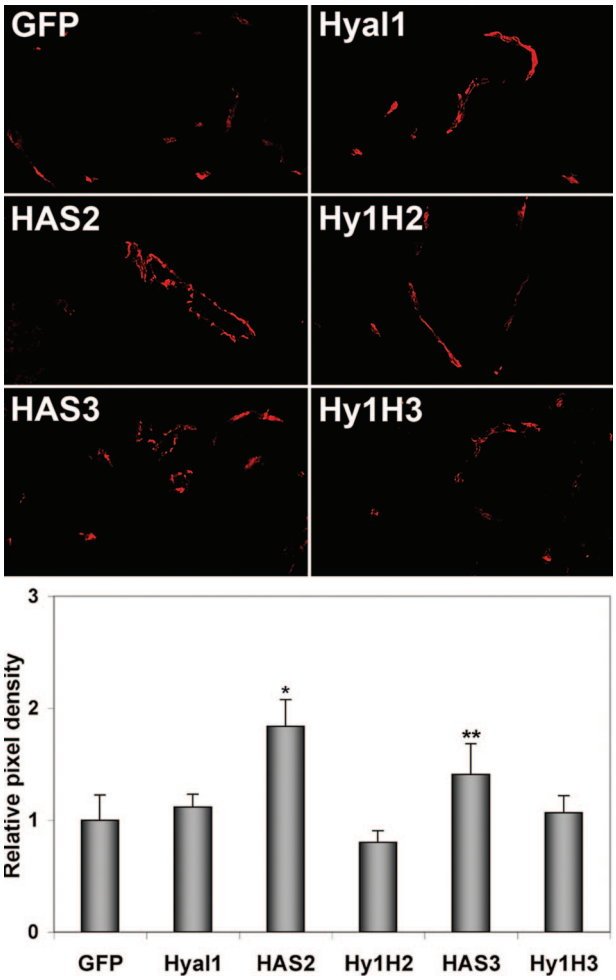

Figure 3. Enhanced tumorigenesis in the prostate does not correlate with intratumoral blood vessel density. Orthotopic tumors were embedded in OCT compound and cryosectioned. Sections were stained with anti-CD31-PE conjugate and 10 randomly selected sections per tumor were digitally photographed under a fluorescence microscope at ×400 magnification with a 5-second exposure time. Representative images from each tumor type as indicated are shown. Images were processed as indicated in Materials and Methods to obtain total vessel area per section as pixel density. Mean pixel density per section ± SEM is plotted for 10 sections of three different tumors per group; $^{*}P < 0.01$, $^{**}P < 0.05$.

and were more numerous per unit area than in the HA-rich tumors.

After tumor removal from the sacrificed mice, para-aortic lymph node metastases were visualized by near infrared optical imaging (Figure 4). Representative images of lymph nodes *in situ* were captured (Figure 4A) before excision of the nodes. *Ex vivo* images were then collected (Figure 4, B and D) and used to quantify node fluorescence as a measure of metastatic burden in mice injected with each cell line. Results were confirmed by histological staining of sectioned nodes from each animal in the study (Figure 4, C and E). Fluorescence intensity of the nodes was quantified and normalized to that of the nodes from the GFP control group (Figure 4F). As we previously found, overexpression of Hyal1 alone induced metastasis of nonmetastatic 22Rv1 cells. However, co-expression of either HAS isozyme with Hyal1 significantly increased size and total fluorescence of lymph nodes by a further 2.3-fold (HAS2, $P < 0.01$) or 1.7-fold (HAS3, $P < 0.01$). Therefore, the combined expression of Hyal1 and HAS provides a synergistic stimulus for prostate tumor growth and metastasis.

To determine mechanisms underlying the observed changes *in vivo*, we investigated aggressive tumor correlate behaviors *in vitro*. We previously found that HAS3 stable overexpression induced changes in cell surface integrin levels that resulted in compromised adhesion of the cells to extracellular matrix proteins.[14] This is one mechanism by which HAS expression may suppress cell growth in the absence of sufficient hyaluronidase activity. Because impaired adhesion has the potential to impact apoptosis, cell-cycle progression, and cell motility, we examined these characteristics of the transfectants. Asynchronous populations of the transfectant cell lines were analyzed by propidium iodide staining and flow cytometry. Percentages of cells in each phase of the cell cycle, as well as the fraction of cells undergoing apoptosis, were quantified and compared for each cell line. Results were plotted for a representative assay (Figure 5A). The most striking points observed in these data were that cells overexpressing Hyal1 alone exhibited an increase from ≈18 to ≈30% in S phase (DNA synthesis), whereas the G_0/G_1 (resting) phase fraction is similarly reduced. The intrinsic rate of Hyal1 transfectant proliferation is ≈50% faster than GFP control-transfected cells, which is consistent with a higher level of DNA synthesis and shorter overall doubling time. Concurrent expression of Hyal1 with HAS3 also significantly increased the fraction of S phase cells, consistent with restoration of their proliferative rates in culture and acceleration of tumor growth kinetics *in vivo*. Surprisingly, Hyal1/HAS2 co-expressing cells were not significantly different from controls. No appreciable differences in the apoptotic fraction were observed among the cell lines.

To investigate cell cycle alterations more carefully, we performed a time course analysis of cell cycle re-entry after synchronization of the cells with the mitotic arrest agent, nocodazole. Comparison of Hyal1 transfectants to GFP controls (Figure 5, B and C) showed a significantly shorter time in G_0/G_1 resting phase, ≈6 to 7 hours versus 12 to 14 hours, with consequent accelerated advance to S phase. HAS2 (Figure 5B) transfectants did not exhibit significantly different characteristics. It was evident that the Hyal1/HAS2 co-expressing cells failed to synchronize completely so the effect of co-expression on specific phases of the cell cycle may be masked. HAS3 transfectants (Figure 5C) advanced to S phase more slowly than controls, ≈16 to 18 hours. Hyal1/HAS3 co-transfectants, although entering S phase at a similar rate to controls, exhibited an S phase peak of comparable magnitude to the Hyal1 cells. Thus, excess HA production has the potential to extend time in the resting phase, whereas Hyal1 expression appears to reduce this time and accelerate overall cell cycling.

Finally, we examined cell adhesion and motility in response to the extracellular matrix protein collagen IV, a normal component of the prostate basement membrane. To assay adhesion, tumor cell suspensions were applied to collagen-coated microwell plates (Figure 6A). HAS2-

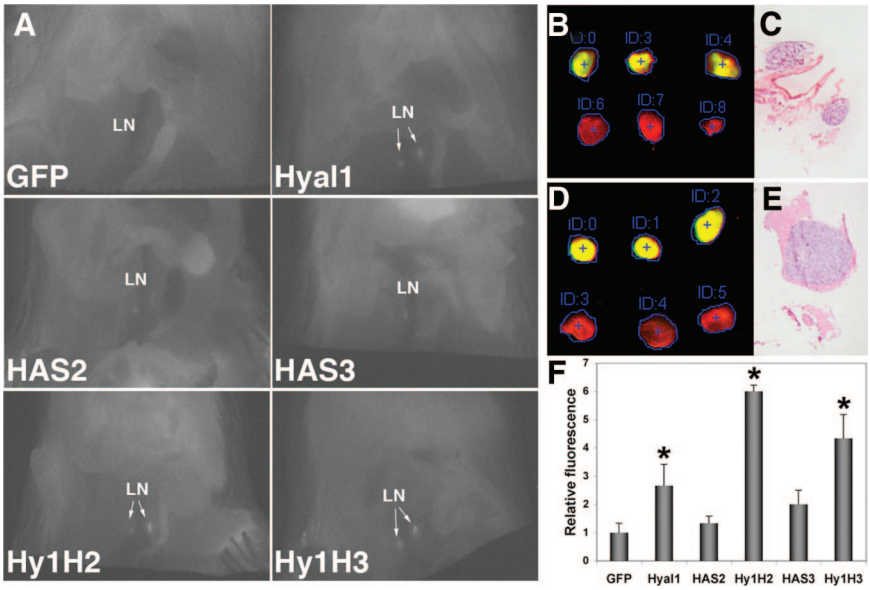

Figure 4. Spontaneous lymph node metastasis is initiated by Hyal1 and potentiated by HAS/Hyal1 co-expression. Three days before study termination, mice were injected intravenously with IRDye 800CW EGF (1 nmol). After final image capture, animals were sacrificed and dissected to expose the para-aortic lymph nodes. **A:** Images of lymph nodes *in situ* from representative animals are shown for comparison at the same look-up table. LN indicates position of lymph nodes; **arrows** indicate fluorescence in the lymph nodes. Excised lymph nodes from all animals in the study were imaged intact for fluorescence quantification (**B**, **D**) and sectioned for histology (**C**, **E**). Nodes shown are from animals injected with HAS2 (**B**, **C**) and Hyal1/HAS2 (**D**, **E**) transfectants. **F:** Fluorescence intensity (800 channel signal with signal-to-noise ratio >3) of all excised nodes was normalized to fluorescence of nodes from mice injected with control GFP transfectants. Mean ± SEM is plotted; $^*P < 0.01$.

and HAS3-overexpressing cells, which bear abundant pericellular HA relative to untransfected, Hyal1-transfected, or Hyal1/HAS-co-transfected cells, were ≈50% less adherent to this substrate. In similar assays, the HAS transfectants were up to 80% less adherent on fibronectin- or laminin-coated plates (not shown). Reduced adhesion is one likely explanation for the slower growth rate of these cells *in vitro*, but is not necessarily coupled to intrinsic cell motility. To test this, we assayed migration of the cells in a modified Boyden chamber (Figure 6B). Migration of the HAS transfectants was modestly but significantly reduced relative to the GFP controls. Strikingly, although Hyal1 individual and Hyal1/HAS-co-transfected cells adhered comparably to GFP control transfectants, cell migration of Hyal1 transfectants was significantly increased, and further enhanced by Hyal1/HAS co-expression. Results of the cell migration assay directly reflected the pattern of metastatic potential exhibited. Collectively, results of our characterizations *in vivo* and *in vitro*, summarized in Table 1, implicate Hyal1 expression in enhanced tumor cell intrinsic motility, as well as proliferation, and demonstrate that the combined production of HA with the Hyal1-processing enzyme maximizes this potential.

Discussion

Unfavorable prognosis for invasive prostate cancer is strongly correlated with the combined presence of HA and Hyal1 in human resected prostate tumor tissue. Independently, overexpression of either Hyal1 or HAS has been previously implicated in promotion of subcutaneous tumorigenesis in mice.[16,23–25] However, the respective importance of HA synthesis and processing enzymes in prostatic tumor growth kinetics and metastatic potential has not been evaluated. In this study, we found that HAS expression modestly suppressed prostate tumor cell growth at the orthotopic site, whereas the combined production of HA with excess Hyal1-processing activity served to accelerate primary tumor growth kinetics (Table 1). The expression of Hyal1 alone was sufficient to initiate spontaneous lymph node metastasis while having no effect on primary tumor size, but the simultaneous overproduction of HA further accelerated tumor cell dissemination. We demonstrated these differential effects were independent of tumor angiogenesis. Rather, they were attributable to altered cell-cycle progression in the presence of Hyal1 alone, and to increased motility stimulated by Hyal1 but significantly enhanced by co-expression of HAS with Hyal1. This is the first study to dissect the respective roles of the HA synthesis and processing enzymes in an orthotopic prostate cancer progression model and to correlate with underlying cellular mechanisms.

Tumor cell responses to HA synthesis have been reported by a number of groups. Several studies have found HAS overexpression promotes tumorigenesis[23] or anchorage-independent growth,[26] whereas others found metastatic frequency increased without impacting tumorigenesis.[27,28] Interestingly, many studies have also shown that large HA quantities of high molecular mass (ie, >100 kDa) are antiproliferative and antiangiogenic,[29,30] capable of suppressing growth of both tumor cells[16,31] and vascular endothelial cells.[31] These responses are dependent on both size and concentration of HA. In fact, dose dependence of HA production was shown by selection of tumor cells for different levels of HAS1 overexpression, which promoted subcutaneous tumorigenesis at low levels while suppressing it at high levels.[32] However, it is clear that the turnover of HA is critical for the observed phenotypic outcome of excess HA synthesis. HAS was tumorigenic in gliomas only if cells expressed hyaluronidase.[31] In breast cancer cell lines, expression of HAS2 and the hyaluronidase isozyme Hyal2 were associated with invasive phenotype.[33] In our previous work, antisense HAS suppression inhibited sub-

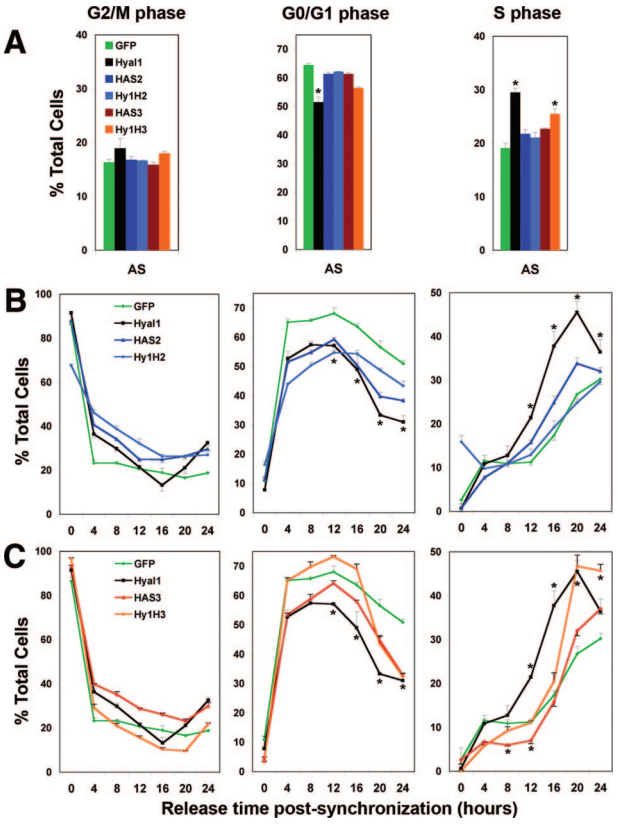

Figure 5. Cell-cycle analysis reveals accelerated cell cycling of Hyal1-overexpressing cells. Transfectant cell lines were fixed, permeabilized, propidium iodide-stained, and analyzed by flow cytometry. **A:** Respective mean percentages of cells in each phase of the cycle are plotted ± SEM for a total of three experiments in asynchronous cultures. Cells were synchronized in the G_2/M phase by nocodazole treatment, then released by replacement with standard medium for the indicated times and similarly analyzed by flow cytometry. Mean ± SEM of triplicate assays is plotted for each phase of the cell cycle at each time point as indicated at the top of each column; $^*P < 0.01$. Plots compare HAS2 (dark blue triangles), Hyal1 (black squares), and Hyal1/HAS2 (light blue circles) cells (**B**) or HAS3 (red triangles), Hyal1 (black squares), and Hyal1/HAS3 (orange circles) cells (**C**).

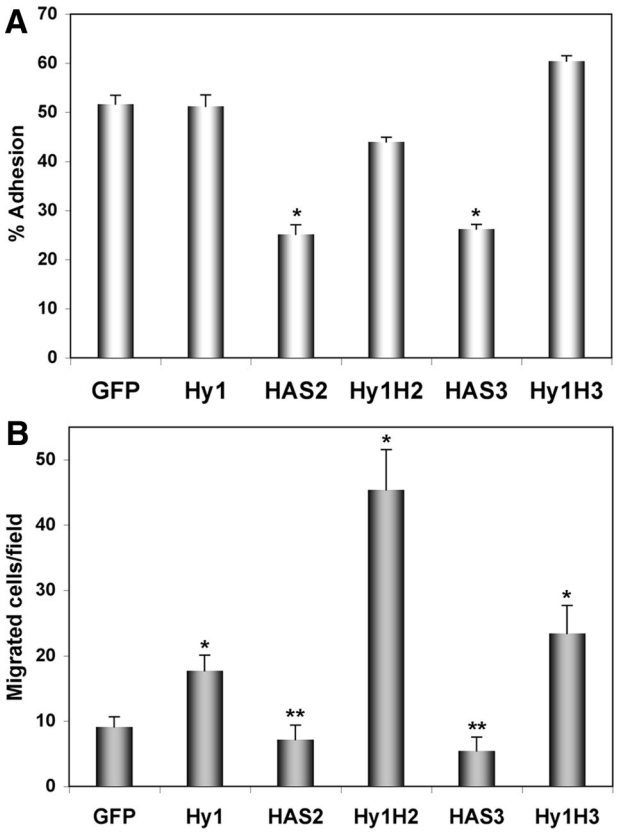

Figure 6. Cell adhesion and migration to collagen are impaired by HAS expression but migration is increased synergistically with Hyal1 and HAS co-expression. **A:** Cell adhesion to type IV collagen (5 μg/ml) was quantified in a precoated 96-well plate, to which calcein-labeled tumor cell suspensions were added. Nonadherent cells were removed by gentle washing after a 2-hour incubation at 37°C. Remaining adherent cells were lysed and the fluorescence of each well was normalized to a standard curve for each cell line. Results plotted are the mean ± SEM of quadruplicate wells from a total of three experiments; $^*P < 0.01$. **B:** Cell migration was assayed in a modified Boyden chamber. Stably transfected 22Rv1 cells as indicated were trypsin-released and resuspended in serum-free RPMI. The lower wells of the chamber contained type IV collagen (25 μmol/L) in serum-free RPMI. Cells (20,000/well) were placed in quadruplicate wells of the upper chamber, separated from the lower wells by a polycarbonate membrane with 8 μm pore size. After 20 hours of incubation at 37°C, membranes were fixed and stained. Migrated cells were counted in five random fields per well at ×150 magnification. Average number of cells per field is plotted ± SEM for each cell line; $^*P < 0.01$, $^{**}P < 0.05$.

cutaneous growth of tumor cells that could be restored by HA supplementation.[19] In addition, concurrent overexpression of Hyal1 and HAS2 increased tumor size several fold relative to either Hyal1 or HAS alone.[16] Collectively, these results are consistent with our observations in the work presented here. Importantly, we demonstrate that the excess production of HA is growth suppressive to the cells synthesizing it, whereas the simultaneous elevation of turnover by Hyal1 provides a growth-promoting signal.

HA turnover by Hyal1 may provide an oligomeric HA signal in the extracellular space[34] that would compete with polymers for receptor binding at the cell surface. Alternatively or in addition, Hyal1 may function in concert with Hyal2 to enhance tumor cell reuptake of HA polymers,[35] with the majority of degradation taking place intracellularly. We have quantified expression of other hyaluronidase isozymes, including Hyal2, and found that although Hyal2 and Hyal3 messages are present, they do not show differential expression among human prostate tumor cell lines and their expression did not change with any of our gene manipulations (M.A. Simpson, unpublished), nor are there any reports of their clinical involvement in prostate cancer. Presumably, these enzymes are participating to an equal extent in the phenomena we have examined here.

Altered receptor engagement subsequent to cellular stimulation by HA polymers versus HA oligosaccharides influences signaling pathways for cellular transformation and apoptosis.[5] For example, targeted disruption of the HAS2 gene in mice supports the implication of HA as an essential signal for epithelial to mesenchymal transition that precedes cardiac septal formation.[36] This function of HA as a transformation signal has been demonstrated in cancer progression as well, in which case neoplastic transformations may be promoted by HA-mediated activation of receptor tyrosine kinases such as ErbB2.[37–39] Constitutive engagement of HA receptors by small amounts of newly synthesized HA polymers was shown to stimulate cell cycling through assembly of protein com-

Table 1. Summary of Transfectant Prostate Tumor Cell Characteristics

	GFP	Hyal1	HAS2	Hy1/H2	HAS3	Hy1/H3
Tumorigenesis	1	1.00	0.43*	6.24*	0.80*	2.03*
Metastasis	1	2.67*	1.32	6.00*	1.55	4.33*
Blood vessel density	1	1.11	1.84*	0.81	1.41	1.07
Apoptosis	No significant differences, <5% total cells					
Proliferation	1	1.62*	0.10*	1.14	0.54*	1.00
Cell cycle						
Asynchronous (S phase)		+12%				+7%
Time to S phase re-entry	12 to 14 hours	6 to 8 hours	12 hours	NA	16 to 18 hours	14 to 16 hours
Adhesion	1	0.99	0.49*	0.85	0.51*	1.15
Migration	1	1.95*	0.78*	5.00*	0.60*	2.57*

*$P < 0.05$ relative to GFP control.
NA, not fully arrested.

plexes including PI3-kinase, cdc37, and the cytoskeletal adaptor ezrin.[39,40] In addition, HA responses are context-dependent with respect to two-dimensional versus three-dimensional culture conditions.[4] Anchorage-independent growth of prostate tumor cells requires HA polymer ligation of cell surface receptors to stabilize cytoskeletal architecture by intracellular association with ankyrin, ezrin, cytoskeletal proteins, and other adaptors.[40,41] These interactions have been successfully disrupted and shown to induce tumor apoptosis *in vitro* and *in vivo* by administration of HA oligosaccharides.[40,42]

A component of HA signaling in transformation may be its influence on cell-cycle progression through physical processes. Pericellular HA matrices enlarge during mitotic cell rounding and this cell-associated HA deposition facilitates de-adhesion during the G_2/M phase of the cell cycle.[43] Intracellular HA was detectable and appeared to interact with the mitotic spindle throughout cell division. The authors postulated that its extrusion to the cytoplasm could be needed to exert steric or osmotic effects on trafficking of intracellular components. Using metastatic Dunning rat prostate tumor cells, Koike and colleagues[44] observed that HA production may be induced in tumor cells by increasing mechanical stress as the tumor enlarges, contributing to survival and anchorage- independent spheroidal growth of the tumor cells. We previously found that exogenously added *Streptomyces* hyaluronidase could relieve the growth inhibition imposed by overproduction of HA.[14] Consistent with our observations in the current study, Hyal1 isolated from plasma was previously shown to promote cell cycling, evidenced by increased cells in the DNA synthesis (S) phase with reduced numbers in the resting (G_0/G_1) phase[45]; also, G_2/M arrest is the outcome of Hyal1 knockdown.[26] We have further shown here that overproduction of HA (but not exogenous HA addition) lengthens the duration of G_0/G_1 and delays S phase entry. Collectively, these results are consistent with a model in which HA is required both within the tumor cell to physically facilitate accelerated progression through mitosis, and at the pericellular surface to permit cell morphology changes essential to division. In this model, excess HA unbalanced by the turnover activity of Hyal1 would inhibit processes such as chromosomal condensation and/or DNA synthesis, possibly by steric or electrostatic interference, thus slowing entry into G_0/G_1. The presence of Hyal1 may relieve HA inhibition through enhanced clearance if sufficiently expressed to balance synthesis.

An additional explanation for altered tumorigenesis and metastasis in conditions of HA dysregulation is that HA antagonizes cell adhesion and motility. Excess HA accumulation at the cell surface impairs integrin-mediated adhesion, so migration is also affected, because cells must adhere and de-adhere to orchestrate nonrandom movements. In part because of its anti-adhesive function but also as a result of receptor engagement, HA has a prominent role in promoting cell migration. Pericardial explants from HA-deficient mice, which did not undergo endothelial cell migration needed for cardiac morphogenesis, were shown to have restored motility in the presence of exogenous HA or dominant-negative ras.[36] Thus, HA can serve as a ras-dependent signal for cell migration. A similar role for HA in genitourinary development was shown by monitoring prostate ductal branching in embryonic explants.[46] In renal proximal tubular epithelial cells, HA directly stimulates migration through MAP kinase activation[47] and also suppresses the anti-migratory transforming growth factor-β1 signal normally produced by the cells.[48] Pericellular HA synthesis in response to prostate fibroblast-conditioned media has been observed to correlate with increased migration of prostate tumor cells,[49] where HA was most densely deposited at the trailing edge of the polarized motile cells, consistent with its potential role in de-adhesion. However, the overexpression of HAS isozymes has also been shown to reduce motility,[50] as we have seen in the current report. In neither of these prior cases was hyaluronidase activity investigated, however, so it is probable that HA turnover differed among the cells tested, and that such differences contribute to the net effect of HA production on cell motility. This notion is supported by our findings of dramatically increased motility in the Hyal1/HAS transfectants: cells continually synthesize the anti-adhesive surface HA, but because they rapidly turn it over, streaming and reattachment during movement are not hindered.

In summary, our finding that cell adhesion and motility are, respectively, restored and enhanced by concurrent elevation of HA synthesis and HA turnover enzymes supports the implication of HA in suppressed adhesion, growth, and migration of tumor cells. Thus, the observation of HA accumulation within tumor tissue is not neces-

sarily an intrinsic negative prognostic factor and its presence alone is not carcinogenic. In particular, we have consistently found that effects of HA on growth and motility are dependent on cells synthesizing the HA, and cannot be recapitulated with exogenous addition of HA to cultures or assays. Rather, the subsequent or concurrent infusion of hyaluronidase, regardless of cellular origin, leads to accelerated tumor growth and metastatic spread that is potentiated in the presence of excess HA production. We propose that more rapid cell cycling and proliferation underlie Hyal1-mediated metastasis, whereas Hyal1/HAS co-transfectants are metastatic because of enhanced motility, independently of any potential effects on tumor angiogenesis. Motility is not increased as a result of altered extracellular matrix adhesion, but may result from differential use of adhesion receptors. Because exogenous, extracellular hyaluronidase *in vitro* and in subcutaneous tumors also acts on tumor-borne HA, the results collectively imply that prostate tumor epithelial and stromal cells must both be targeted in therapeutic strategies involving inhibition of HA production or turnover.

Acknowledgment

We thank Dr. Joseph Barycki for critical evaluation of the manuscript.

References

1. Pienta KJ, Smith DC: Advances in prostate cancer chemotherapy: a new era begins. CA Cancer J Clin 2005, 55:300–318
2. Fraser JR, Laurent TC, Laurent UB: Hyaluronan: its nature, distribution, functions and turnover. J Intern Med 1997, 242:27–33
3. Stern R: Hyaluronan metabolism: a major paradox in cancer biology. Pathol Biol (Paris) 2005, 53:372–382
4. Toole BP: Hyaluronan promotes the malignant phenotype. Glycobiology 2002, 12:37R–42R
5. Toole BP: Hyaluronan: from extracellular glue to pericellular cue. Nat Rev Cancer 2004, 4:528–539
6. Rooney P, Kumar S: Inverse relationship between hyaluronan and collagens in development and angiogenesis. Differentiation 1993, 54:1–9
7. Aaltomaa S, Lipponen P, Tammi R, Tammi M, Viitanen J, Kankkunen JP, Kosma VM: Strong stromal hyaluronan expression is associated with PSA recurrence in local prostate cancer. Urol Int 2002, 69:266–272
8. Auvinen P, Tammi R, Parkkinen J, Tammi M, Agren U, Johansson R, Hirvikoski P, Eskelinen M, Kosma VM: Hyaluronan in peritumoral stroma and malignant cells associates with breast cancer spreading and predicts survival. Am J Pathol 2000, 156:529–536
9. Ekici S, Cerwinka WH, Duncan R, Gomez P, Civantos F, Soloway MS, Lokeshwar VB: Comparison of the prognostic potential of hyaluronic acid, hyaluronidase (HYAL-1), CD44v6 and microvessel density for prostate cancer. Int J Cancer 2004, 112:121–129
10. Lokeshwar VB, Obek C, Soloway MS, Block NL: Tumor-associated hyaluronic acid: a new sensitive and specific urine marker for bladder cancer [published erratum appears in Cancer Res 1998 Jul 15; 58(14):3191]. Cancer Res 1997, 57:773–777
11. Posey JT, Soloway MS, Ekici S, Sofer M, Civantos F, Duncan RC, Lokeshwar VB: Evaluation of the prognostic potential of hyaluronic acid and hyaluronidase (HYAL1) for prostate cancer. Cancer Res 2003, 63:2638–2644
12. Ricciardelli C, Mayne K, Sykes PJ, Raymond WA, McCaul K, Marshall VR, Horsfall DJ: Elevated levels of versican but not decorin predict disease progression in early-stage prostate cancer. Clin Cancer Res 1998, 4:963–971
13. Noordzij MA, van Steenbrugge GJ, Verkaik NS, Schroder FH, van der Kwast TH: The prognostic value of CD44 isoforms in prostate cancer patients treated by radical prostatectomy. Clin Cancer Res 1997, 3:805–815
14. Bharadwaj AG, Rector K, Simpson MA: Inducible hyaluronan production reveals differential effects on prostate tumor cell growth and tumor angiogenesis. J Biol Chem 2007, 282:20561–20572
15. Kovar JL, Johnson MA, Volcheck WM, Chen J, Simpson MA: Hyaluronidase expression induces prostate tumor metastasis in an orthotopic mouse model. Am J Pathol 2006, 169:1415–1426
16. Simpson MA: Concurrent expression of hyaluronan biosynthetic and processing enzymes promotes growth and vascularization of prostate tumors in mice. Am J Pathol 2006, 169:247–257
17. Simpson MA, Reiland J, Burger SR, Furcht LT, Spicer AP, Oegema TR, Jr., McCarthy JB: Hyaluronan synthase elevation in metastatic prostate carcinoma cells correlates with hyaluronan surface retention, a prerequisite for rapid adhesion to bone marrow endothelial cells. J Biol Chem 2001, 276:17949–17957
18. Simpson MA, Wilson CM, Furcht LT, Spicer AP, Oegema TR, Jr., McCarthy JB: Manipulation of hyaluronan synthase expression in prostate adenocarcinoma cells alters pericellular matrix retention and adhesion to bone marrow endothelial cells. J Biol Chem 2002, 277:10050–10057
19. Simpson MA, Wilson CM, McCarthy JB: Inhibition of prostate tumor cell hyaluronan synthesis impairs subcutaneous growth and vascularization in immunocompromised mice. Am J Pathol 2002, 161:849–857
20. Wild R, Ramakrishnan S, Sedgewick J, Griffioen AW: Quantitative assessment of angiogenesis and tumor vessel architecture by computer-assisted digital image analysis: effects of VEGF-toxin conjugate on tumor microvessel density. Microvasc Res 2000, 59:368–376
21. Lokeshwar VB, Rubinowicz D, Schroeder GL, Forgacs E, Minna JD, Block NL, Nadji M, Lokeshwar BL: Stromal and epithelial expression of tumor markers hyaluronic acid and HYAL1 hyaluronidase in prostate cancer. J Biol Chem 2001, 276:11922–11932
22. West DC, Hampson IN, Arnold F, Kumar S: Angiogenesis induced by degradation products of hyaluronic acid. Science 1985, 228: 1324–1326
23. Kosaki R, Watanabe K, Yamaguchi Y: Overproduction of hyaluronan by expression of the hyaluronan synthase Has2 enhances anchorage-independent growth and tumorigenicity. Cancer Res 1999, 59:1141–1145
24. Liu N, Gao F, Han Z, Xu X, Underhill CB, Zhang L: Hyaluronan synthase 3 overexpression promotes the growth of TSU prostate cancer cells. Cancer Res 2001, 61:5207–5214
25. Lokeshwar VB, Cerwinka WH, Isoyama T, Lokeshwar BL: HYAL1 hyaluronidase in prostate cancer: a tumor promoter and suppressor. Cancer Res 2005, 65:7782–7789
26. Bullard KM, Kim HR, Wheeler MA, Wilson CM, Neudauer CL, Simpson MA, McCarthy JB: Hyaluronan synthase-3 is upregulated in metastatic colon carcinoma cells and manipulation of expression alters matrix retention and cellular growth. Int J Cancer 2003, 107:739–746
27. Itano N, Sawai T, Miyaishi O, Kimata K: Relationship between hyaluronan production and metastatic potential of mouse mammary carcinoma cells. Cancer Res 1999, 59:2499–2504
28. Delpech B, Laquerriere A, Maingonnat C, Bertrand P, Freger P: Hyaluronidase is more elevated in human brain metastases than in primary brain tumours. Anticancer Res 2002, 22:2423–2427
29. Rooney P, Kumar S, Ponting J, Wang M: The role of hyaluronan in tumour neovascularization. Int J Cancer 1995, 60:632–636
30. West DC, Kumar S: The effect of hyaluronate and its oligosaccharides on endothelial cell proliferation and monolayer integrity. Exp Cell Res 1989, 183:179–196
31. Enegd B, King JA, Stylli S, Paradiso L, Kaye AH, Novak U: Overexpression of hyaluronan synthase-2 reduces the tumorigenic potential of glioma cells lacking hyaluronidase activity. Neurosurgery 2002, 50:1311–1318
32. Itano N, Sawai T, Atsumi F, Miyaishi O, Taniguchi S, Kannagi R, Hamaguchi M, Kimata K: Selective expression and functional characteristics of three mammalian hyaluronan synthases in oncogenic malignant transformation. J Biol Chem 2004, 279:18679–18687
33. Udabage L, Brownlee GR, Nilsson SK, Brown TJ: The over-expres-

sion of HAS2, Hyal-2 and CD44 is implicated in the invasiveness of breast cancer. Exp Cell Res 2005, 310:205–217
34. Lokeshwar VB, Rubinowicz D, Schroeder GL, Forgacs E, Minna JD, Block NL, Nadji M, Lokeshwar BL: Stromal and epithelial expression of tumor markers hyaluronic acid and HYAL1 hyaluronidase in prostate cancer. J Biol Chem 2001, 276:11922–11932
35. Harada H, Takahashi M: CD44-dependent intracellular and extracellular catabolism of hyaluronic acid by hyaluronidase-1 and -2. J Biol Chem 2007, 282:5597–5607
36. Camenisch TD, Spicer AP, Brehm-Gibson T, Biesterfeldt J, Augustine ML, Calabro A, Jr., Kubalak S, Klewer SE, McDonald JA: Disruption of hyaluronan synthase-2 abrogates normal cardiac morphogenesis and hyaluronan-mediated transformation of epithelium to mesenchyme. J Clin Invest 2000, 106:349–360
37. Misra S, Toole BP, Ghatak S: Hyaluronan constitutively regulates activation of multiple receptor tyrosine kinases in epithelial and carcinoma cells. J Biol Chem 2006, 281:34936–34941
38. Toole BP, Zoltan-Jones A, Misra S, Ghatak S: Hyaluronan: a critical component of epithelial-mesenchymal and epithelial-carcinoma transitions. Cells Tissues Organs 2005, 179:66–72
39. Ghatak S, Misra S, Toole BP: Hyaluronan constitutively regulates ErbB2 phosphorylation and signaling complex formation in carcinoma cells. J Biol Chem 2005, 280:8875–8883
40. Ghatak S, Misra S, Toole BP: Hyaluronan oligosaccharides inhibit anchorage-independent growth of tumor cells by suppressing the phosphoinositide 3-kinase/Akt cell survival pathway. J Biol Chem 2002, 277:38013–38020
41. Zhu D, Bourguignon LY: The ankyrin-binding domain of CD44s is involved in regulating hyaluronic acid-mediated functions and prostate tumor cell transformation. Cell Motil Cytoskeleton 1998, 39: 209–222
42. Zeng C, Toole BP, Kinney SD, Kuo JW, Stamenkovic I: Inhibition of tumor growth in vivo by hyaluronan oligomers. Int J Cancer 1998, 77:396–401
43. Evanko SP, Wight TN: Intracellular localization of hyaluronan in proliferating cells. J Histochem Cytochem 1999, 47:1331–1342
44. Koike C, McKee TD, Pluen A, Ramanujan S, Burton K, Munn LL, Boucher Y, Jain RK: Solid stress facilitates spheroid formation: potential involvement of hyaluronan. Br J Cancer 2002, 86:947–953
45. Lin G, Stern R: Plasma hyaluronidase (Hyal-1) promotes tumor cell cycling. Cancer Lett 2001, 163:95–101
46. Gakunga P, Frost G, Shuster S, Cunha G, Formby B, Stern R: Hyaluronan is a prerequisite for ductal branching morphogenesis. Development 1997, 124:3987–3997
47. Ito T, Williams JD, Al-Assaf S, Phillips GO, Phillips AO: Hyaluronan and proximal tubular cell migration. Kidney Int 2004, 65:823–833
48. Ito T, Williams JD, Fraser D, Phillips AO: Hyaluronan attenuates transforming growth factor-beta1-mediated signaling in renal proximal tubular epithelial cells. Am J Pathol 2004, 164:1979–1988
49. Ricciardelli C, Russell DL, Ween MP, Mayne K, Suwiwat S, Byers S, Marshall VR, Tilley WD, Horsfall DJ: Formation of hyaluronan- and versican-rich pericellular matrix by prostate cancer cells promotes cell motility. J Biol Chem 2007, 282:10814–10825
50. Brinck J, Heldin P: Expression of recombinant hyaluronan synthase (HAS) isoforms in CHO cells reduces cell migration and cell surface CD44. Exp Cell Res 1999, 252:342–351